Research Article GU J Sci 38(1): x-x (2025) DOI: 10.35378/gujs.1451314

Gazi University

Journal of Science

http://dergipark.gov.tr/gujs

Theoretical Investigations on Vic-Dioxime Complexes Coordinated with Cu(II) and Ni(II) Ions: Using Density Functional Theory

Berna CATIKKAS*

Hatay Mustafa Kemal University, Department of Physics, 31000 Antakya, Hatay, Türkiye.

Highlights

- Theoretical investigations for *Vic*-Dioxime metal (Cu^{II} and Ni^{II} ions) complexes.
- An analysis of the molecular orbital descriptors and molecular orbitals.
- Density of states diagrams (DOS and PDOS), nonlinear optic effect (NLO) and infrared spectroscopy.

Article Info

Received: 12 Mar 2024
Accepted: 25 Oct 2024

Keywords

Vicinal dioxime complexes, Molecular orbital descriptors, Infrared spectra, DFT

Abstract

Metal complexes containing vic-dioximes are currently of interest due to their diverse properties and potential applications in various chemical processes, including medicine, where they serve as well-known antimicrobial agents, biology, catalysis, electrochemical sensors, and metallurgy. A vicinal dioxime ligand coordinated with Cu^{II} and Ni^{II} ions complexes were studied by using Density Functional Theory methods by using Gaussian 09. The optimized ground state structures of the complexes were calculated with mPW1PW91 iop(3/76=0572004280) method. Different basis sets have been selected for each atom as follows: Sulphur: cc-pVQZ, Carbon and Hydrogen: 6-31+G(d,p), Nitrogen: 6-31+G(2d), Oxygen: cc-pVQZ and Metal: Copper/Nickel: SDDALL, SDD. The both complexes have achieved fully optimized ground state geometries characterized by square planar structures surrounding the central metal atoms. Based on the molecular orbital descriptor values, the hardness is determined to be 1.60 eV for [Cu(II)L_2] and 1.47 eV for [Ni(II)L_2] complexes, respectively. Both complexes show considerable potential for use in nonlinear optics applications.

1. INTRODUCTION

Extensive studies have been carried out on transition metal complexes that incorporate vicinal dioxime ligands and this topic has been thoroughly reviewed in multiple publications [1–7]. The amphoteric nature of vicinal dioximes originates from the existence of moderately acidic hydroxyl groups and marginally basic nitrogen atoms, facilitating their formation of square-planar complexes resembling the corrin type with metals, copper (II) and nickel (II) as central atoms. Vicinal dioximes and their metal complexes are presently attracting attention because of their physicochemical properties, patterns of reactivity, and potential applications in numerous significant chemical processes. These encompass fields such as medicine, biology, bioorganic systems [8, 9], catalytic processes, electrochemical and electro-optical sensors, and semiconductor characteristics [1–7, 10, 11], as well as metallurgy. *Vic*-dioxime complexes have found widespread applications across diverse fields due to their exceptional stability. They are well-suited as representatives for emulating B_{12} vitamin and function well as efficient chelating agents in the examination of trace metals [12, 13].

In recent years, computational studies employing quantum mechanics have been documented in the literature, focusing on the biological properties of *vic*-dioxime and Cu(II)-Ni(II) complexes [14, 15]. Nevertheless, comprehensive investigations utilizing Density Functional Theory (DFT) for *vic*-dioxime with copper and nickel complexes are currently absent in the literature, particularly with regards to detailed structural and electronic analyses of the title complexes.

* e-mail: berna@mku.edu.tr

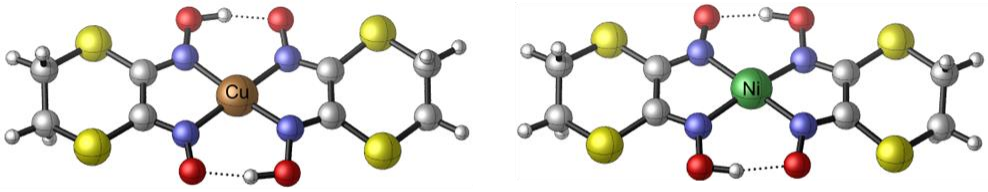

[Cu(II)L_2] **[Ni(II)L_2]**

Figure 1. *3D structure of the complexes in gas phases*

The research previously presented in the form of a comprehensive proceeding during the second IKSTC-2023 Çankırı Karatekin University Conference elucidated the ligand L= (2Z,3Z)-1,4-dithiane-2,3-dionedioxime conformations, molecular orbital characteristics, and nonlinear effects. This ongoing investigation aims to examine the electronic properties of complex compounds (Figure 1). Previous studies have not theoretically investigated the determination of structure of the complexes. Quantum mechanical hybrid methods were employed to calculate theoretical geometric parameters, density of states, chemical properties, molecular electrostatic surface (MEP) maps, nonlinear optical effects (NLO), and ground state vibration modes.

2. MATERIAL METHOD

2.1. Experimental

The Fourier Transform Infrared (FTIR) spectra of the studied complexes were captured using a Perkin Elmer Spectrum Two FTIR (equipped with a U-ATR) in the range of 450 to 4000 cm^{-1}. The molar conductivities of the complexes were observed at room temperature in DMSO (approximately 10^{-3} M) by using a conductivity meter, Jenway Model (4070).

2.2. Computation Details

Density Functional Theory computations were conducted by using the Gaussian 16 [16]. The complexes in its ground state (in gas phase conditions) were optimized using density functional theory, specifically employing the mPW1PW91 methods [17] with iop(3/76=0572004280). Different basis sets have been selected for each atom as follows: Sulphur: cc-pVQZ, Carbon and Hydrogen: 6-31+G(d,p), Nitrogen: 6-31+G(2d), Oxygen: cc-pVQZ and Metal: Copper/Nickel: SDDALL, SDD. Consistency was maintained across all calculations such as frontier molecular orbital properties, (TDOS, PDOS), MEP, NLO and vibrations were calculated using at this specified level. Molecular structures obtained from computations were visualized using the CYLview program [18] (Figure 1) and GausView 6 [19] program.

Molecular orbital density of states (total and partial DOS) were calculated using GaussSum 2.2 [20] to compute the group contributions. The partitioning of groups and percentage such as C=N, O-H, metal and other atoms has been carried out.

In order to investigate and acquire information concerning regions of diverse charge distribution within the molecule, theoretical calculations were utilized to analyse the electrostatic potential. V(r) is determined based on the electronic density function provided below, Z_A represents the charge associated with the nucleus A is situated at position R_A [21–23]

$$V(r) = \sum_A \frac{Z_A}{(R_A - r)} - \int \frac{\rho(r')}{(r' - r)} d(r'). \quad (1)$$

The expressions for μ: dipole moment, α_{tot}: polarizability and β_{tot}: first order hyper polarizability of the investigated complexes are articulated in terms of i, j, k = x, y, z coordinates, as denoted by the following equations:

$$\mu = \left(\mu_x{}^2 + \mu_y{}^2 + \mu_z{}^2\right)^{1/2} \quad (2)$$

$$\alpha_{tot} = 1/3\left(\alpha_{xx} + \alpha_{yy} + \alpha_{zz}\right) \quad (3)$$

$$\beta_i = \beta_{iii} + \beta_{ijj} + \beta_{ikk} \quad (4)$$

$$\beta_{tot} = \left(\beta_x + \beta_y + \beta_z\right)^{1/2}. \quad (5)$$

3. THE RESEARCH FINDINGS AND DISCUSSION

3.1. Structural Aspects

The transition-metal complexes of these vicinal dioximes predominantly exhibit N,N-coordination in a square planar configuration [24–27]. The complexes exhibit that two ligand molecules are coordinated to a Cu(II) or Ni (II) metal ion in an equatorial position with a perfect square planar coordination environment ($\tau = 0$ in Table 1). Structures with a central atom coordinated by vicinal-dioxime ligands and containing Cu^{2+} and Ni^{2+} ions have been recorded with a square planar geometry in the literature [28–33] Optimized 3D structures of the complexes were given with atomic numbering in Figure 2. These calculations indicate that the optimized structure conforms to a square planar geometry (in Figure 2). Based on the computed structural parameters, the N-M-N angles (M = Ni or Cu) are determined to be 82 degrees and 98 degrees. The experimental measured conductivity values being close to zero (3-6 μ simens) indicate that the optimized geometries of the complexes are square planar.

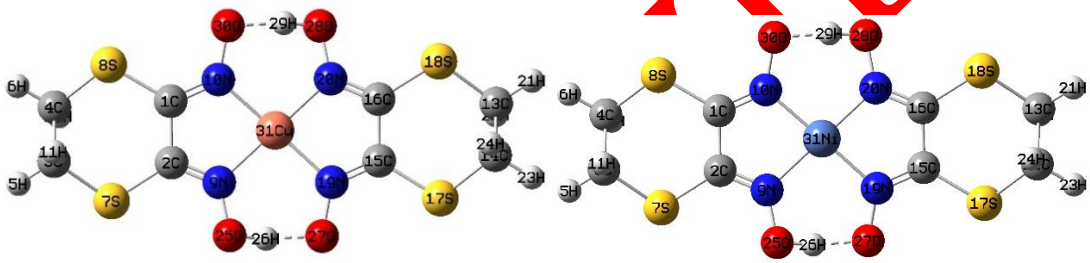

Figure 2. *3D structure of [Cu(II)L₂] and [Ni(II)L₂] complexes*

When comparing the bond lengths between the complexes [Cu(II)L_2] and [Ni(II)L_2], it is observed that the M-N bond length is shorter in the [Cu(II)L_2] complex than [Ni(II)L_2] (Table 1). The investigation revealed that the stability of the complexes conforms to the Irving-Williams series, with Cu(II) demonstrating superior stability compared to Ni(II) [34]. In the literature, the M-N: M= Ni(II) and Pd (II) bond length within the square planar coordination of vicinal-dioxime ligands in crystal structures has been reported as 1.978(3) Å and 1.970(3) Å for Pd (II) [35]. In this study, the metal-nitrogen bond length was calculated as 1.94 and 1.95 Å. The C_{16}-S_{18} and C_{13}-S_{18} bond lengths are the same in both complexes. The N_{20}-O_{28} and O_{28}-H_{29} bond lengths are very similar. However, the O_{30}-H_{29} hydrogen bond lengths are shorter in the [Cu(II)L_2] complex.

Table 1. *Computed geometric parameters of the complexes*

M=Cu(II), Ni(II)	**[Cu(II)L_2]**	**[Ni(II)L_2]**
Bond length (Å)		
M-N	1.94	1.95
C_1-N_{10}	1.29	1.30
C_1-C_2	1.48	1.47
C_{16}-S_{18}	1.73	1.73
C_{13}-S_{18}	1.80	1.80
N_{20}-O_{28}	1.34	1.35
O_{28}-H_{29}	1.00	0.99
O_{30}-H_{29} (H-Bond)	1.64	1.71
Bond angel (Å)		
N-M-N	82	82
N-M-N	98	98
Dihedral angle τ (^{0})		
τ (C_1-C_2-C_{15}-C_{16})	0	0
τ (N_9-N_{10}-N_{20}-N_{19})	0	0

3.2. Calculation of Molecular Reactivity

The HOMO and LUMO, along with their associated properties like energy, are highly valuable as they represent the primary orbitals involved in reactions. The energy differential between HOMO and LUMO provides crucial insights for understanding molecular electrical conductivity properties and evaluating electron conductivity. In the Cu (II) and Ni (II) complex, unpaired electrons in the HOMO and LUMO orbitals lead to their division into alpha (α) and beta (β) orbits, resulting in distinct energy levels for these spin orbitals due to their multiplicity. Figures 3 and 4 illustrates that the HOMO & LUMO surfaces, along with the total electron density surfaces (where red indicates the highest negative potentials and most electron-rich areas, and blue denotes electron-poor regions), are predominantly localized around all metal (M), carbon (C), nitrogen (N), and sulphur (S) atoms, with hydrogen atoms being excluded from this concentration. Based on these findings, the electronic transitions observed in [Cu(II)L_2] and [Ni(II)L_2] complex, arising from the excitation of electrons from the HOMO to the LUMO, are identified as n→π* and π→π* transitions. As seen, $\Delta E_{HOMO\text{-}LUMO}$ was calculated as -3.19 eV (α) and -2,90 eV (β) for [Cu(II)L_2]. The energy differences between α and β orbits are 1.05 and 0.99 eV, respectively. The $\Delta E_{HOMO\text{-}LUMO}$ was determined to be -2.93 eV (α) and -2.13 eV (α) for [Ni(II)L_2], respectively. A large HOMO–LUMO gap ($\Delta E = E_{LUMO} - E_{HOMO}$) is commonly associated with enhanced kinetic stability and reduced chemical reactivity [36]. The fact that the energy difference (ΔE) of the Cu-ion complex is greater than that of the Ni-ion complex indicates that the Cu complex is more stable than the Ni complex.

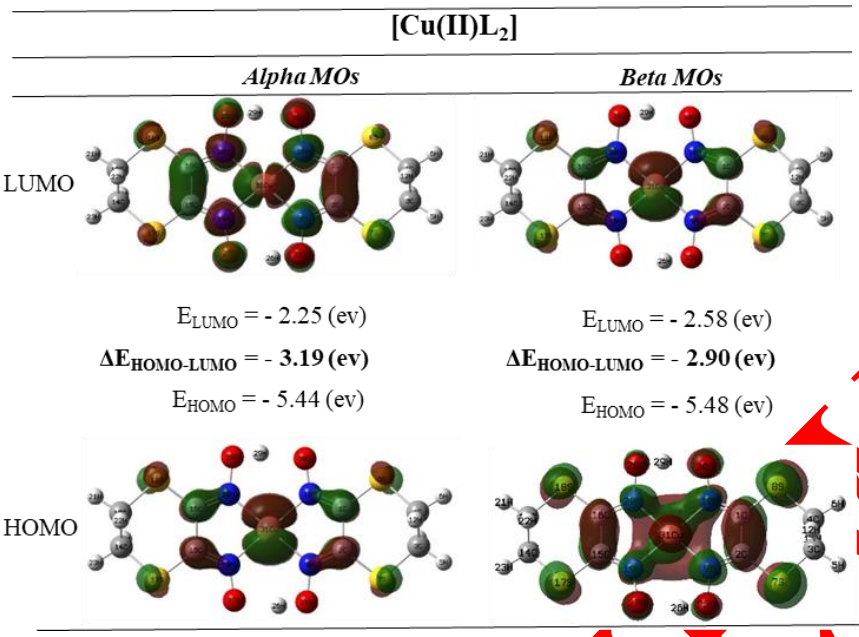

Figure 3. *Molecular orbitals and energies of the [Cu(II)L₂] complexes*

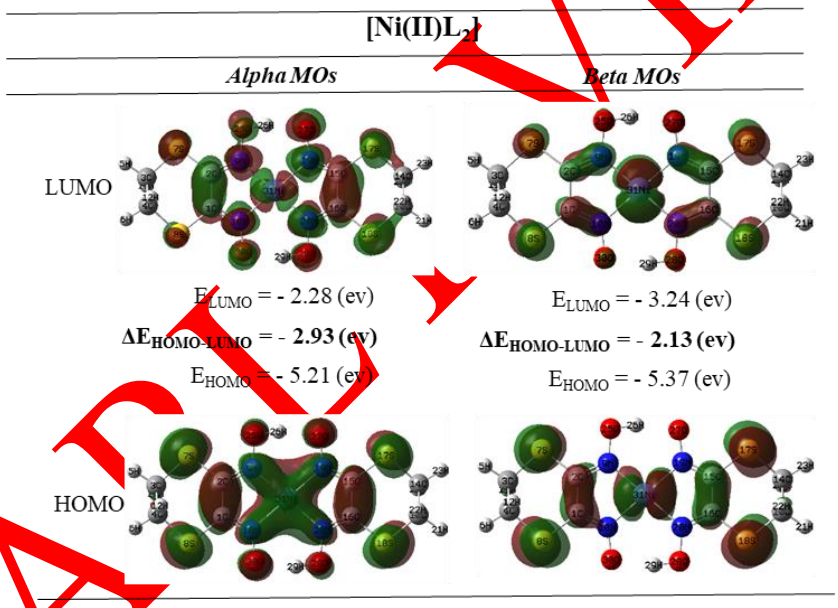

Figure 4. *Molecular orbitals and energies of the [Ni(II)L₂] complexes*

Properties derived from HOMO-LUMO calculations prove beneficial for analyzing molecular reactivity, particularly within the realms of organic synthesis and the biomedical field [37]. Koopman's theorem allows for the definition of chemical potential: $\mu=(E_{HOMO}+E_{LUMO})/2$, chemical hardness: $\eta=(E_{HOMO}-E_{LUMO})/2$), global softness: $S=1/\eta$, electronegativity: $\chi=-\mu$ and electrophilicity index: $\omega=\mu^2/2\eta$ when applied to closed-shell molecules [38,39].

The HOMO and LUMO orbital energies can be used to define the ionization potential ($-E_{HOMO}$) and electron affinity ($-E_{LUMO}$). In terms of chemical hardness, a substantial HOMO–LUMO gap denotes a molecule with high hardness, whereas a minimal HOMO–LUMO gap indicates a molecule with low hardness [40]. As seen in the Table 2, chemical hardness (η) is 1.60 eV and 1.47 eV (alpha), 1.45 eV and 1.07 eV (beta). for the [Cu(II)L_2] and [Ni(II)L_2], respectively. As evidenced by the molecular orbital descriptor values, it is observed that the ligands exhibit a greater affinity towards Ni ions compared to Cu ions (Table 2). Ionisation potential (IP) is 5.44 eV and 5.21 eV (alpha), 5.48 eV and 5.37 eV (beta) for the

[Cu(II)L_2] and [Ni(II)L_2], respectively.

Table 2. *Computed energy values of molecular orbital descriptors for the complexes*

Molecular Properties (eV)	**[Cu(II)L_2]**		**[Ni(II)L_2]**	
	alpha	beta	alpha	beta
E_{LUMO}	-2.25	-2.58	-2.28	-3.24
E_{HOMO}	-5.44	-5.48	-5.21	-5.37
$\Delta E_{HOMO-LUMO}$	**-3.19**	**-2.90**	**-2.93**	**-2.13**
Ionisation Potential (IP)	**5.44**	**5.48**	**5.21**	**5.37**
Electron Affinity (EA)	2.25	2.58	2.28	3.24
Chemical Hardness (η)	**1.60**	**1.45**	**1.47**	**1.07**
Electronegativity (χ)	3.84	4.03	3.74	4.31
Chemical Potential (μ)	-3.84	-4.03	-3.74	-4.31
Softness (S) eV^{-1}	**0.63**	**0.69**	**0.68**	**0.94**
Electrophilicity index (ω)	4.63	5.60	4.77	8.70

.

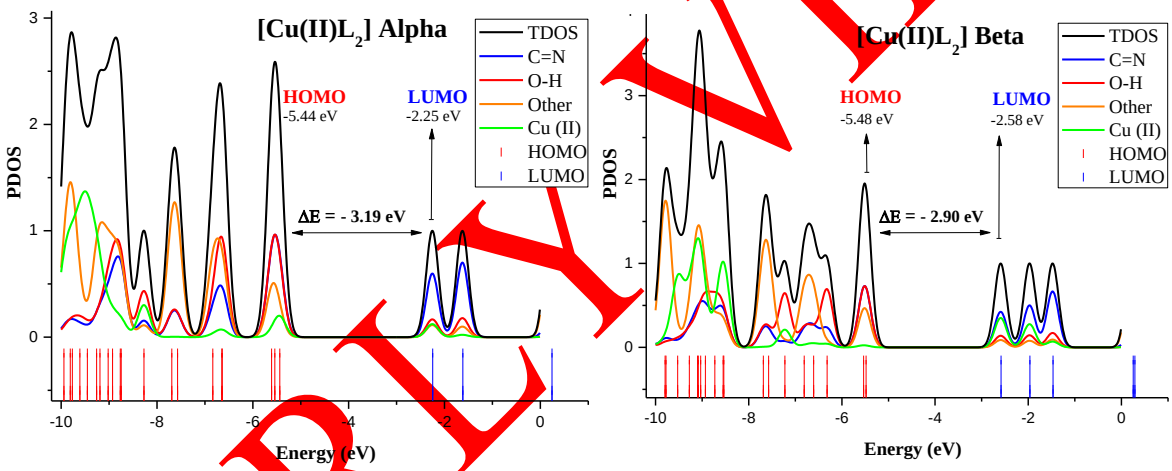

Figure 5. *Density of states diagrams (PDOS and TDOS) for the [Cu(II)L_2] complexes*

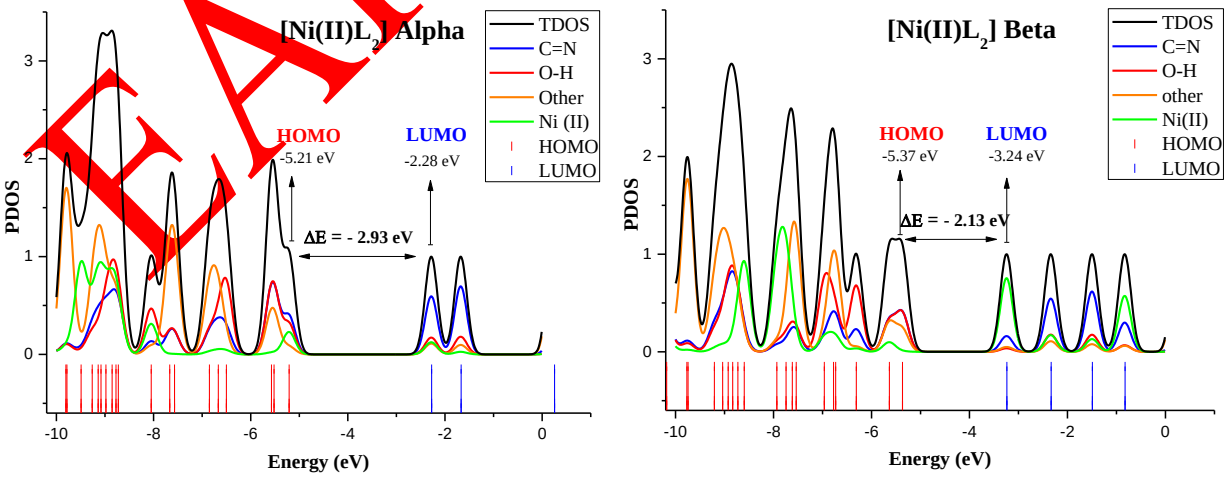

Figure 6. *Density of states diagrams (PDOS and TDOS) for the [Ni(II)L_2] complexes*

The graph of PDOS showed in Figures 5 and 6 were generated using the Gauss-Sum 2.2 program. They show a visual depiction of the compositions of molecular orbitals (MO) and their roles in chemical bonding.

As can be seen in the Table 3, the LUMO orbitals are predominantly localized on the C=N (60%, 59%) regions of the complexes. Conversely, the HOMO primarily localizes on the orbitals of C=N and O-H groups. Additionally, the contribution of frontier molecular orbitals (FMO) from metals and other atoms is relatively diminished in comparison.

Table 3. *The percentage of calculated PDOS contribution for the studied complexes*

	[Cu(II)L$_2$]					**[Ni(II)L$_2$]**			
	C=N	O-H	Cu (II)	Other		C=N	O-H	Ni (II)	Other
Alpha					Alpha				
LUMO	60	17	12	11	LUMO	59	17	12	11
HOMO	39	35	19	8	HOMO	39	31	23	8
Beta					Beta				
LUMO	42	14	9	35	LUMO	16	4	5	75
HOMO	37	40	23	0	HOMO	39	38	22	1

3.3. Calculation of Molecular Electrostatic Potential (MEP) Surface

To predict attacks, it is necessary to identify reactive sites by electrophiles and nucleophiles on the investigated compounds, molecular electrostatic potential (MEP) a visual tool to comprehend the molecule's relative polarity. The graphical representation of chemically reactive areas, like the negative areas (in red) is associated with electrophilic reactivity, while nucleophilic reactivity is linked to positive areas (in blue).

Figure 7 shows that the oxygen (-0.089 a.u.) for [Ni(II)L$_2$] atoms exhibit the highest negative potential within the examined complexes, whereas the hydrogen and carbon atoms of the compound carry positive potentials. The light yellow region distributed around the sulfur atom signifies its electronegative character. MEP of the examined complexes reveals that the areas containing a negative potential are situated around the electronegative atom, specifically the oxygen atom. As anticipated, the metal atoms are positioned above regions exhibiting positive potential. Quantum computational calculations reveal that the Cu(II) complex displays a positive electrostatic potential across most of its surface, in contrast to the Ni(II) complex. Representation of MEPSs of the copper complex in Figure 7 showed that the copper atom (+0.144 a.u.) at the center of the [Cu(II)L$_2$] complex is more positively charged than the [Ni(II)L$_2$] complex.

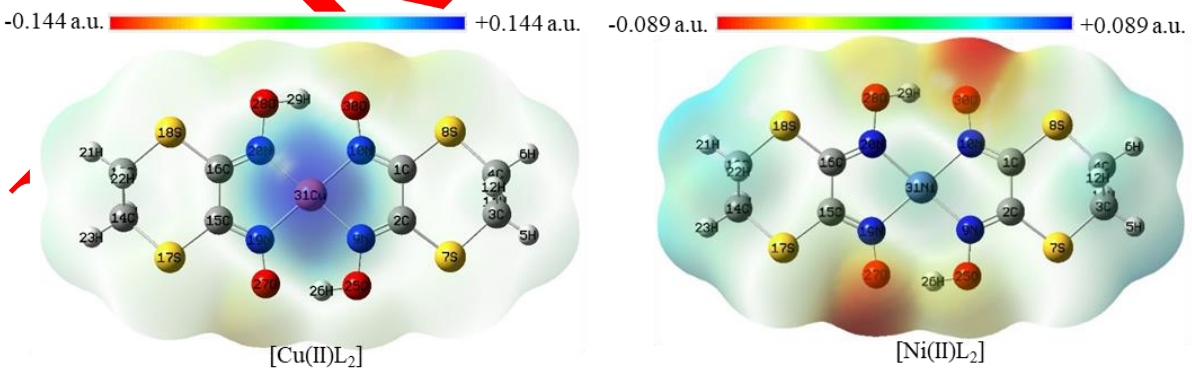

Figure 7. *Molecular electrostatic potential mapping for the investigated complexes*

3.4. Calculation of Nonlinear Optics Properties

The parameters of dipole moment (μ), polarizability (α), anisotropy of polarizability (Δα), first-order static hyperpolarizability (β₀), and second-order hyperpolarizability (γ) provide important information about nonlinear optical (NLO) properties. NLO properties of molecules are closely linked to the behavior of delocalized π-electrons, as well as the characteristics of donor-acceptor groups and the energy gap between

the highest occupied molecular orbital (HOMO) and the lowest unoccupied molecular orbital (LUMO). These molecular features influence the electronic response to external electric fields and are fundamentally associated with key parameters such as the static dipole moment (μ), the average linear polarizability (α_{tot}), and the first hyperpolarizability (β_{tot}). Computational studies play a crucial role in quantifying these parameters, offering insights into the electronic structure and providing predictive models for the NLO behavior of materials.

Computed values of the dipole moments (μ), average polarizabilities ($\Delta\alpha_{tot}$) and first order hyper-polarizabilities (β_{tot}) were listed in Table 4. The measurements were conducted in electrostatic units (esu), employing conversion factors of 0.1482×10^{-24} esu for polarizability (α) and 8.63922×10^{-33} esu for first-order hyper-polarizability (β) per atomic unit (a.u.). Table 4 clearly demonstrates that the μ, α and β is impacted by the value of x-axis. The optical energy gap is an important measurement in assessing charge transfer [41]. As the optical gap diminishes, the first hyper-polarizability values increase due to the enhanced facilitation of electronic charge transfer. The [Cu(II)L_2] complex exhibits a greater energy value than the [Ni(II)L_2] complex (in Table 4), with lower polarizability and hyper-polarizability values compared to the [Ni(II)L_2] complex (Table 4). Both complexes show promise as potential candidates for application in nonlinear optics contexts.

Table 4. *The computed NLO parameters*

μ&α	**[Cu(II)L_2]**	**[Ni(II)L_2]**	**β**	**[Cu(II)L_2]**	**[Ni(II)L_2]**
μ_x	0.015	0.019	β_{xxx}	296.37	205.83
μ_y	0.003	0.010	β_{xxy}	29.71	230.15
μ_z	-0.044	0.024	β_{xyy}	14.27	2.85
μ (D)	**0.044**	**0.028**	β_{yyy}	-18.69	19.39
α_{xx}	413.07	462.15	β_{xxz}	-29.89	-375.41
α_{xy}	-0.37	-1.37	β_{xyz}	-12.97	-72.65
α_{yy}	239.96	245.25	β_{yyz}	4.63	-12.03
α_{xz}	-0.17	0.12	β_{xzz}	-14.54	23.75
α_{yz}	-2.12	1.90	β_{yzz}	-0.05	7.08
α_{zz}	121.68	123.01	β_{zzz}	-6.05	-33.23
<α> (au)	**258.24**	**276.80**	β_x	296.10	232.43
Δα (au)	**759.15**	**853.96**	β_y	10.97	256.62
Δa ($\times 10^{-23}$ esu)	**11.25**	**12.66**	β_z	-31.31	-420.67
			β_{tot} (a.u.)	**297.95**	**544.84**
			β_{tot} ($\times 10^{-31}$ esu)	**25.74**	**47.07**

3.5. Infrared Spectroscopy

Calculated and experimental vibrational bands of the complexes are given in Table 5 and shown observed infrared spectrum bands in Figures 9-11. A strong absorption is observed in the region of 3650-2570 cm^{-1} for the O-H stretching vibration of oximes [42]. Therefore, they are located in the same region as the CH and OH peaks. This overlap in the spectral region suggests potential interactions or similarities in the vibrational modes associated with these functional groups, which could complicate the precise assignment of individual peaks in the infrared spectrum. The vibrational spectra reveal O-H stretching peaks are observed 3212 cm^{-1} and 3134 cm^{-1} for the ligand, an O-H stretching peak at 3317 cm^{-1} for the [Cu(II)L_2] complex, and peak at 3321 cm^{-1} for the [Ni(II)L_2] complex. Due to the formation of new O-H bonds in the complexes, the O-H stretching vibrations in the complexes have increased compared to the ligand. CH vibrations are observed at 2975 cm^{-1} and 2861 cm^{-1} for the ligand, 2989 cm^{-1} for the [Cu(II)L_2] complex, and at 3091 cm^{-1} and 3060 cm^{-1} for the [Ni(II)L_2] complex in the infrared spectrums (in Figures 10 and 11.) and 3091 cm^{-1} for the [Ni(II)L_2] complex. The shift in C-H stretching vibrations has occurred in the direction of increasing frequency.

Typically, imines exhibit C=N stretching vibrations in the range of 1690-1640 cm^{-1} [42,43]. In a previous study utilizing experimental infrared spectroscopy to investigate a Cu(II) complex with a dioxime ligand in a square planar configuration featuring an O...H bridge bond, closely resembling the structure examined in the current research, the characteristic C=N stretching vibrations were observed within the range of 1610 to 1560 cm^{-1} [29]. The C=N stretching frequencies are observed at 1610 cm^{-1} and 1578 cm^{-1} for ligand, 1622 cm^{-1} and 1527 cm^{-1} for [Cu(II)L_2], and 1643 cm^{-1} and 1561 cm^{-1} for [Ni(II)L_2].

Oximes exhibit a prominent band around 960-930 cm^{-1}, which is attributed to the stretching vibration of the N-O bond. The typical range for this vibrational band is between 1030 and 870 cm^{-1} [42]. The N-O vibrations are observed at 1011 cm^{-1}, 955 cm^{-1}, 919 cm^{-1} for the ligand, 1086 cm^{-1}, 1067 cm^{-1}, 1007 cm^{-1}, 971 cm^{-1} for [Cu(II)L_2], 1083 cm^{-1}, 1067 cm^{-1}, 1006 cm^{-1}, 968 cm^{-1} for [Ni(II)L_2] complexes.

IR vibrations of C-S stretching are generally occur within the spectral range of 715-570 cm^{-1} [42]. The C-S vibrations are observed at the following ranges: 722-550 cm^{-1} for the ligand, 749-559 cm^{-1} for [Cu(II)L_2], and 743-515 cm^{-1} for [Ni(II)L_2].

The vibrational frequencies of Metal-Nitrogen stretching for metal complexes could not be determined as they fall below the region of 600-300 cm^{-1} [44]. In previous experimental studies, the M-N vibrations of dioxime complexes were recorded in the infrared spectrum, with the Cu-N stretching vibration ν(Cu-N) observed at 511 cm^{-1} and the Ni-N stretching vibration ν(Ni-N) at 503 cm^{-1} [45]. For [Cu(II)L_2], the M-N stretching frequencies are observed at 512 cm^{-1}, 483 cm^{-1}, and 465 cm^{-1}, while for [Ni(II)L_2], they are observed at 515 cm^{-1}, 509 cm^{-1}, and 486 cm^{-1}. These frequency values suggest slight differences in the metal-nitrogen bond strengths between copper and nickel complexes.

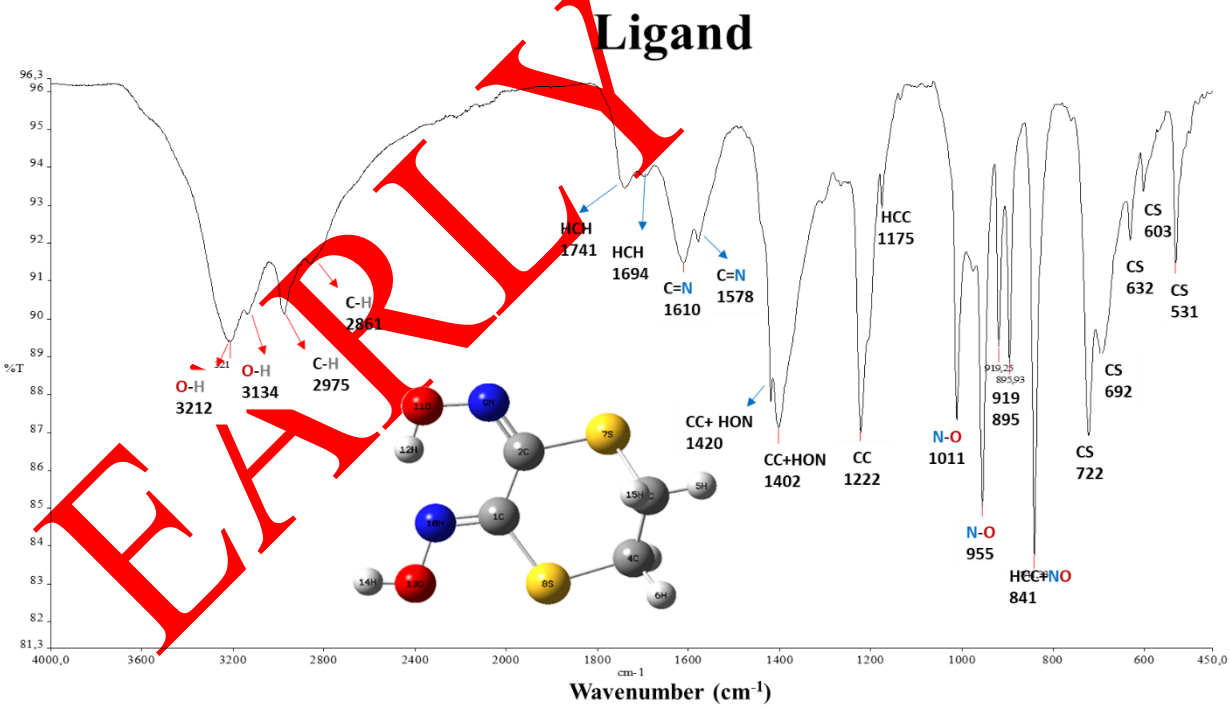

Figure 9. *Infrared spectrum of the ligand*

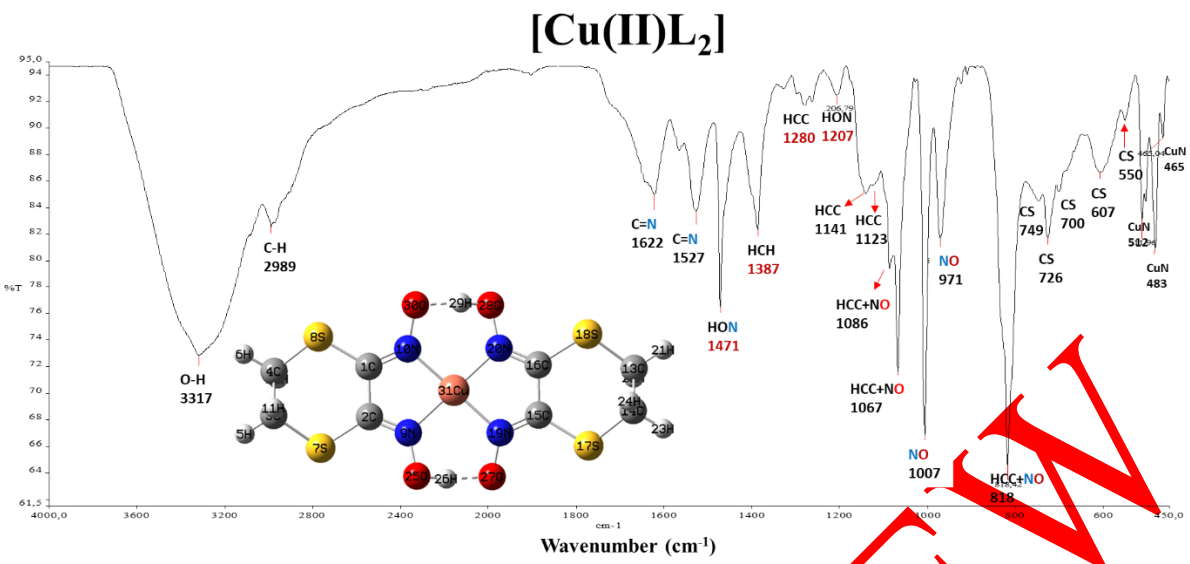

Figure 10. *Infrared spectrum of the [Cu(II)L₂]*

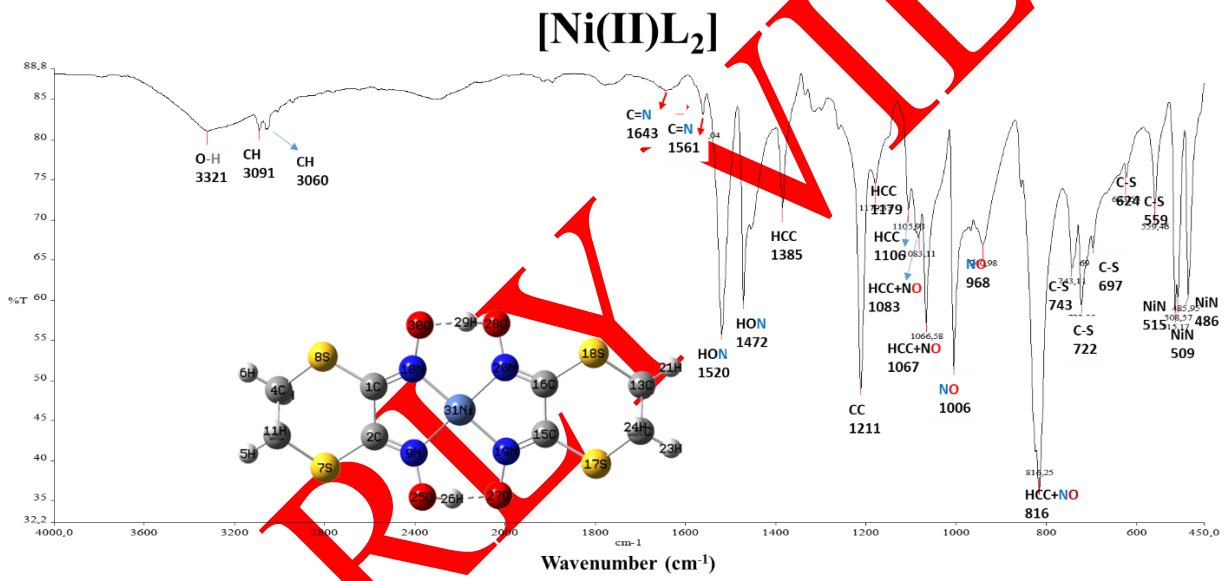

Figure 11. *Infrared spectrum of the [Ni(II)L₂]*

Table 5. *Computed and experimental vibrational wavenumbers (cm⁻¹), along with their corresponding assignments, for the [Cu(II)L₂] and [Ni(II)L₂] complexes*

		[Cu(II)L₂]			[Ni(II)L₂]			
No		**Cal^{Freq}**	**I^{IR}**	**Exp^{Freq}**	**Cal^{Freq}**	**I^{IR}**	**Exp^{Freq}**	**Assignment**
1	A	16	2		16	2		τCNNC
2	A	26	0		35	1		τSCCS
3	A	49	0		47	1		τCNNC
4	A	61	1		60	2		δCSC
5	A	69	5		67	3		δCSC
6	A	82	1		85	2		νMN
7	A	92	7		90	5		νMN
8	A	108	1		110	1		νMN
9	A	133	5		132	5		νMN
10	A	162	0		158	0		νMN

11	A	173	0		174	0		νMN
12	A	179	0		185	1		τHOMN
13	A	194	1		209	1		τCNMN
14	A	247	0		246	0		τCNMN
15	A	255	19		253	23		νO...H
16	A	258	0		261	0		νO...H
17	A	266	11		264	7		νO...H
18	A	271	1		271	0		τHCCH
19	A	279	2		278	6		τHCCH
20	A	286	3		286	3		νO...H
21	A	306	5		302	0		νO...H
22	A	311	1		312	26		τHCCH
23	A	323	0		323	1		τONCS
24	A	340	0		333	3		νMN
25	A	351	165		351	117		νMN
26	A	362	5		359	1		δNMN+δCCS
27	A	375	33		377	6		δNMN+δCCS
28	A	433	8		427	13		νCC+νCS
29	A	441	8		432	39		τHCCH
30	A	461	1		462	0		τHCCH
31	A	468	11	465	469	8	486	νMN
32	A	502	6	483	509	3	509	νMN
33	A	509	1	512	521	0	515	νMN
34	A	577	1		583	1		τSCCS+τNCCN
35	A	590	1	550	595	2	559	τSCCS
36	A	616	0		614	1		νCS
37	A	617	2	607	617	7		νCS
38	A	644	1		645	1	624	νCS
39	A	649	3		650	5		νCS
40	A	709	1	700	691	0	697	νCS
41	A	716	12	726	705	3	722	νCS
42	A	754	0		754	0		νCS
43	A	766	46	749	767	39	743	νCS
44	A	852	7	818	844	76	816	τHCCH
45	A	858	109		850	19		τHCCH
46	A	869	59		856	67		νHO
47	A	878	56		859	84		τHCCH
48	A	909	6		908	4		τHCCH
49	A	914	2		914	1		τHCCH
50	A	923	7		920	9		τHCCH
51	A	930	76		927	93		τHCCH
52	A	989	0	971	987	0	968	νNO
53	A	992	2	1007	991	2	1006	νNO
54	A	1100	160	1067	1085	68	1067	δHCC+νNO
55	A	1113	258	1086	1099	357	1083	δHCC+νNO
56	A	1123	2		1123	2	1106	δHCC+νNO

57	A	1124	2	1141	1124	2		δHCC
58	A	1170	9		1171	7	1179	δHCC
59	A	1172	13		1174	8		δHCC
60	A	1219	37	1207	1226	46	1211	νCC + δHCC
61	A	1227	409		1237	523		νCC
62	A	1260	3		1270	1		νCC+νNO
63	A	1268	39		1274	48		νCC + δHCC
64	A	1281	6		1285	24		νCC+νNO
65	A	1284	4		1289	29		νCO
66	A	1298	11	1280	1299	1		δHCC
67	A	1300	21		1301	8		δHCC
68	A	1419	6	1387	1361	373	1385	δHCC
69	A	1421	9		1378	16		νC=N + δHON
70	A	1426	0		1420	10		νC=N + δHON
71	A	1426	7		1421	7		δHCH
72	A	1432	3		1426	5		δHCH
73	A	1449	329		1426	0		δHCH
74	A	1488	201	1471	1449	385	1472	δHON
75	A	1502	40		1459	58	1520	δHON
76	A	1667	24	1527	1638	25	1561	νC=N + δHON
77	A	1676	43	1622	1645	41	1643	νC=N + δHON
78	A	2725	277		2869	244		νOH
79	A	2782	2970		2912	1609		νOH
80	A	2942	5		2943	5		νCH ssym
81	A	2944	5		2944	6		νCH ssym
82	A	2948	21		2949	22		νCH ssym
83	A	2950	19		2950	17		νCH ssym
84	A	2993	0	2989	2994	0		νCH assym
85	A	2994	1		2994	1	3060	νCH assym
86	A	3006	6		3007	5	3091	νCH assym
87	A	3007	5	3317	3008	5	3321	νOH

Cal^{Freq}: Calculation Frequencies, Exp^{Freq}: Experimental Frequencies

I^{IR} Infrared intensities, ν, stretching; δ, bending; τ, torsion.

4. RESULTS

Consequently, Density Functional Theory investigations were employed to explore the structural and molecular properties of Cu(II) and Ni(II) complexes bearing *vic*-dioxime ligand. The optimized stable geometric structures of the investigated complexes exhibited an approximately square planar configuration surrounding the metal ion at the center within each complexes. Our findings suggest that the examined complexes contain hydrogen bonds between their two hydroxyl (O-H) groups, which are crucial for stabilizing the complexes. The results of the HOMO-LUMO energy gap and ionization potentials indicate that the $[Cu(II)L_2]$ complex is more stable than the $[Ni(II)L_2]$ complex. Both complexes have demonstrated promising potential for applications in the field of nonlinear optics.

CONFLICTS OF INTEREST

No conflict of interest was declared by the author.

ACKNOWLEDGEMENTS

I thank to Cahit Demetgül for providing synthesized complexes. I sincerely thank Gazi University for the opportunities provided to follow the severe earthquake in Antakya-Hatay on February 6, 2023. The numerical calculations reported in this paper were performed at TUBITAK ULAKBIM, High Performance and Grid Computing Center (TRUBA Resources).

REFERENCES

[1] Milios, C. J., Stamatatos, T. C., and Perlepes, S. P., "The Coordination Chemistry of Pyridyl Oximes", Polyhedron, 25: 134–194, (2006).

[2] Smith, A. G., Tasker, P. A., and White, D. J., "The Structures of Phenolic Oximes and Their Complexes", Coordination Chemistry Reviews, 241: 61–85, (2003).

[3] Stynes, D. V, Vernik, I., and Zobi, F., "Iron Complexes of Borylated Vicinal Dioxime Macrocycles", Coordination Chemistry Reviews, 233: 273–287, (2002).

[4] Kukushkin, V. Y. and Pombeiro, A. J. L., "Additions to Metal-Activated Organonitriles", Chemical Reviews, 102: 1771–1802, (2002).

[5] Kukushkin, V. Y., Tudela, D., and Pombeiro, A. J. L., "Metal-Ion Assisted Reactions of Oximes and Reactivity of Oxime-Containing Metal Complexes", Coordination Chemistry Reviews, 156: 333–362, (1996).

[6] Chakravorty, A., "Electroprotic Phenomena and Metal Oxidation States", Comments on Inorganic Chemistry, 4: 1–16, (1985).

[7] Egneus, B., "Investigations of Dioximes and Their Metal Complexes: A Survey of the Literature since 1963", Talanta, 19: 1387–1419, (1972).

[8] Bresciani-Pahor, N., Forcolin, M., Marzilli, L. G., Randaccio, L., Summers, M.F., and Toscano, P.J., "Organocobalt B12 Models: Axial Ligand Effects on the Structural and Coordination Chemistry of Cobaloximes", Coordination Chemistry Reviews, 63: 1–125, (1985).

[9] Pahor, N. B., Dreos, R., Geremia, S., Randaccio, L., Tauzher, G., and Zangrando, E., "Syntheses, Rate Constants, and X-Ray Structures of Alkylrhodoximes with Sigma-Donating Alkyl-Groups Me, Et, and i-Pr. A Comparison with the Analogous Alkylcobaloximes, a Vitamin-B12 Model", Inorganic Chemistry, 29: 3437–3441, (1990).

[10] Chakravorty, A., "Structural Chemistry of Transition Metal Complexes of Oximes", Coordination Chemistry Reviews, 13: 1–46, (1974).

[11] Thomas, T. W. and Underhill, A. E., "Metal–Metal Interactions in Transition-Metal Complexes Containing Infinite Chains of Metal Atoms", Chemical Society Reviews, 1: 99–120, (1972).

[12] Gok, Y. and Kantekin, H., "Synthesis and Characterization of Novel (E, E)-Dioxime and Its Mono- and Heterotrinuclear Complexes", Acta Chemica Scandinavica, 51: 664-671, (1997). DOI: 10.3891/acta.chem.scand.51-0664

[13] Kuse, S., Motomizu, S., and Tôei, K., "O-Diketonedioxime Compounds as Analytical Reagents for the Spectrophotometric Determination of Nickel", Analytica Chimica Acta, 70: 65–76, (1974).

[14] Çalişkan, Ş. G., "DFT, Molecular Docking, Bioactivity and ADME Analyses of Vic-Dioxim Ligand Containing Hydrazone Group and Its Zn (II) Complex", Current Computer-Aided Drug Design, 20:

264–273, (2024).

[15] Çalişkan, Ş. G., Genç, O., Erol, F., and Sarikavakli, N., "Molecular Docking, HOMO-LUMO, Quantum Chemical Computation and Bioactivity Analysis of Vic-Dioxim Derivatives Bearing Hydrazone Group Ligand and Their Ni^{II} and Cu^{II} Complexes", Gazi University Journal of Science Part A: Engineering and Innovation, 9: 299–313, (2022).

[16] Frisch, M. J., Trucks, G. W., Schlegel, H. B., Scuseria, G. E., Robb, M. A., Cheeseman, J. R., Scalmani, G., Barone, V., Petersson, G. A., Nakatsuji, H., Li X., Caricato, M., Marenich, A. V., Bloino, J., Janesko, B. G., Gomperts, R., Mennucci, B., Hratchian, H. P., Ortiz ,J. V., Izmaylov, A. F., Sonnenberg, J. L., Williams-Young, D., Ding, F., Lipparini, F., Egidi, F., Goings, J., Peng, B., Petrone, A., Henderson, T., Ranasinghe, D., Zakrzewski, V. G., Gao, J., Rega, N., Zheng, G., Liang, W., Hada, M., Ehara, M., Toyota, K., Fukuda, R., Hasegawa, J., Ishida, M., Nakajima, T., Honda, Y., Kitao, O., Nakai, H., Vreven, T., Throssell, K., Montgomery, J. A., Jr., Peralta, J. E., Ogliaro, F., Bearpark, M. J., Heyd, J. J., Brothers, E. N., Kudin, K. N., Staroverov, V. N., Keith, T. A., Kobayashi, R., Normand, J., Raghavachari, K., Rendell A. P., Burant J. C., Iyengar S. S., Tomasi J., Cossi M., Millam J. M., Klene, M., Adamo, C., Cammi, R., Ochterski, J. W., Martin, R. L., Morokuma, K., Farkas, O., Foresman, J. B., and Fox D. J., "Gaussian 16, Rev. C.01", Gaussian 16, Rev. C. 01, (2016).

[17] Adamo, C. and Barone, V., "Exchange Functionals with Improved Long-Range Behavior and Adiabatic Connection Methods without Adjustable Parameters: The m PW and m PW1PW Models", The Journal of Chemical Physics, 108: 664–675, (1998).

[18] Legault, C. Y., "CYLview, 1.0b", Université de Sherbrooke, (2009).

[19] Dennington, R., Keith, T. A.., and Millam, J. M., "GaussView 6", Gaussian, (2016).

[20] O'boyle, N. M., Tenderholt, A. L., and Langner K. M., "Cclib: A Library for Package-Independent Computational Chemistry Algorithms", Journal of Computational Chemistry, 29: 839–845, (2008).

[21] Politzer, P., Laurence, P. R., and Jayasuriya K., "Molecular Electrostatic Potentials: An Effective Tool for the Elucidation of Biochemical Phenomena", Environmental Health Perspectives, 61: 191–202, (1985).

[22] Politzer, P. and Murray, J. S., "The Fundamental Nature and Role of the Electrostatic Potential in Atoms and Molecules", Theoretical Chemistry Accounts, 108: 134–142, (2002).

[23] Politzer, P. and Truhlar, D. G., "Chemical applications of atomic and molecular electrostatic potentials: reactivity, structure, scattering, and energetics of organic, inorganic, and biological systems", Springer Science & Business Media, (2013).

[24] Ahsen, V., Musluoğlu, E., Gürek, A., Gül, A., Bekâroğlu, Ö., and Zehnder, M., "Synthesis and Complexation of 1,2-Bis[(Monoaza[15]Crown-5)- N -yl]Glyoxime. Crystal Structure of (1,2-Bis[(Monoaza[15]Crown-5)- N -yl]Glyoximato)Palladium(II)", Helvetica Chimica Acta, 73: 174–179, (1990).

[25] Gul, A. and Bekaroglu, O., "The Synthesis and Complex Formation of 5,6-Dihydrocyclopent [F, G] Acenaphthylene-1,2-Dione Dioxime", Synthesis and Reactivity in Inorganic and Metal-Organic Chemistry, 12: 889–897, (1982).

[26] Gül, A. and Bekâroğlu, Ö., "Synthesis of N, N'-Bis (4'-Benzo [15-Crown-5])-Diaminoglyoxime and Its Complex with Cu (II), Ni (II), Co (II), Pt (II), Pd (II) and UO2 (VI)", Journal of the Chemical Society, Dalton Transactions, 2537: 2537–2541, (1983).

[27] Ertas, M., Ahsen, V., Gül, A., and Bekâroğlu, Ö., "Synthesis of a Novel [10]Ferrocenophanedioxime with Bridge Heteroatoms and of Its Nickel(II) Complex", Journal of Organometallic Chemistry, 335: 105–108, (1987).

[28] Canpolat, E. and Kaya, M., "Synthesis and Characterization of a Vic-Dioxime Derivative and Investigation of Its Complexes with Ni(II), Co(II), Cu(II) and UO2(VI) Metals", Journal of Coordination Chemistry, 55: 961–968, (2002).

[29] Ma, M.S. and Angelici, R.J., "Novel Transition-Metal Complexes of Camphorquinone Dioxime Ligands", Inorganic Chemistry, 19: 363–370, (1980).

[30] Nogheu, L. N., Ghogomu, J. N., Mama, D. B., Nkungli, N. K., Younang, E., and Gadre, S. R., "Structural, Spectral (IR and UV/Visible) and Thermodynamic Properties of Some 3d Transition Metal (II) Chloride Complexes of Glyoxime and Its Derivatives: A DFT and TD-DFT Study", Computational Chemistry, 4: 119, (2016).

[31] Zülfikaroğlu, A., "Quantum Chemical Computational Studies on a Vic-Dioxime Ligand and Its Nickel Complex", Anadolu University Journal of Science and Technology A-Applied Sciences and Engineering, 18: 640–653, (2017).

[32] Babahan, I., Özmen, A., and Aslan, K., "Synthesis and Use of Dioxime Ligands for Treatment of Leukemia and Colon Cancer Cells", Applied Organometallic Chemistry, 31: e3752, (2017).

[33] Coşkun, A., Yılmaz, F., and Akgemci, E. G., "Synthesis, Characterization and Electrochemical Investigation of a Novel Vic-Dioxime Ligand and Its Some Transition Metal Complexes", Journal of Inclusion Phenomena and Macrocyclic Chemistry, 60: 393–400, (2008).

[34] Irving, H. and Williams, Rjp., "637. The Stability of Transition-Metal Complexes", Journal of the Chemical Society (Resumed), 3192–3210, (1953).

[35] Ahsen, V., Musluoğlu, E., Gürek, A., Gül, A., Bekâroğlu, Ö., and Zehnder, M., "Synthesis and Complexation of 1, 2-Bis [(Monoaza [15] Crown-5)-N-yl] Glyoxime. Crystal Structure of (1, 2-Bis [(Monoaza [15] Crown-5)-N-yl] Glyoximato) Palladium (II)", Helvetica Chimica Acta, 73: 174–179, (1990).

[36] Li Y. J., Guo, S. Z., Feng, T., Xie, K. F., and Dong, W. K., "An Investigation into Three-Dimensional Octahedral Multi-Nuclear Ni (II)-Based Complexes Supported by a More Flexible Salamo-Type Ligand", Journal of Molecular Structure, 1228: 129796, (2021).

[37] Zhao, Y. and Truhlar, D. G., "The M06 Suite of Density Functionals for Main Group Thermochemistry, Thermochemical Kinetics, Noncovalent Interactions, Excited States, and Transition Elements: Two New Functionals and Systematic Testing of Four M06-Class Functionals and 12 Other Function", Theoretical Chemistry Accounts, 120: 215–241, (2008).

[38] Koopmans, T., "Über Die Zuordnung von Wellenfunktionen Und Eigenwerten Zu Den Einzelnen Elektronen Eines Atoms", Physica, 1: 104–113, (1934).

[39] Parr, R. G., Szentpály, L. V, and Liu, S., "Electrophilicity Index", Journal of the American Chemical Society, 121: 1922–1924, (1999).

[40] Sheela, N. R., Muthu, S., and Sampathkrishnan, S., "Molecular Orbital Studies (Hardness, Chemical Potential and Electrophilicity), Vibrational Investigation and Theoretical NBO Analysis of 4-4′-(1H-1, 2, 4-Triazol-1-Yl Methylene) Dibenzonitrile Based on Abinitio and DFT Methods", Spectrochimica Acta Part A: Molecular and Biomolecular Spectroscopy, 120: 237–251, (2014).

[41] Mandal, U., Beg, H., and Misra, A., "Effect of Charge Transfer on the First Hyper-Polarizability of N,N-Dimethylaniline and Julolidine: A DFT Based Comparative Study", Journal of Molecular Modeling, 29: 1–15, (2023).

[42] Socrates, G., "Infrared and Raman characteristic group frequencies: tables and charts", John Wiley & Sons, (2004).

[43] Fleming, I. and Williams, D., "Spectroscopic Methods in Organic Chemistry", Springer International Publishing, Cham, (2019).

[44] Nakamoto, K., Morimoto, Y., and Martell, A. E., "Infrared Spectra of Metal Chelate Compounds. IV. Infrared Spectra of Addition Compounds of Metallic Acetylacetonates1a", Journal of the American Chemical Society, 83: 4533–4536, (1961).

[45] Dolaz, M., Tümer, M., Gölcü, A., and Serin, S., "Synthesis and Spectrophotometric Investigation of a New Vic-Dioxime Ligand and Its Transition Metal Complexes", Turkish Journal of Chemistry, 25: 491–500, (2001).